JMEPEG (2022) 31:5706–5711
https://doi.org/10.1007/s11665-022-06673-z

1059-9495/$19.00

TECHNICAL ARTICLE

The Influence of Nb, Zr, and Zr + Hf on the Lattice Parameters and Creep Behavior of β-Solidifying γ-TiAl Alloys

V.M. Imayev, N.Y. Parkhimovich, D.M. Trofimov, and R.M. Imayev

Submitted: 25 June 2021 / Revised: 6 December 2021 / Accepted: 29 January 2022 / Published online: 18 February 2022

X-ray diffraction (XRD) analysis was used to study the effect of alloying with 5 at.% Nb, 5 at.% Zr and 5 at.% (Zr + Hf) on the lattice parameters of the γ(TiAl) and α_2(Ti_3Al) phase in the intermetallic alloys based on Ti-44Al-0.2B (at.%). Before XRD analysis near the same duplex structures were obtained in the alloys under study. The XRD data were used to calculate the tetragonal distortion (c_γ/a_γ) of the γ phase, the $c_{\alpha 2}/a_{\alpha 2}$ ratio of the α_2-phase and the γ/α_2 lattice misfits in the alloys. The c_γ/a_γ ratio and the γ/α_2 lattice misfits were found the highest in the base alloy, followed by the Nb-, (Zr + Hf)- and Zr-containing alloy. The $c_{\alpha 2}/a_{\alpha 2}$ ratio in the alloys was the highest in the Nb-containing alloy, followed by the base alloy and the Zr- and (Zr + Hf)-containing alloy. As was revealed in our previous work, the Ti-44Al-0.2B-based alloys doped with Zr and Zr + Hf demonstrated appreciably higher creep resistance than the alloy doped with Nb and the base alloy. It is assumed that the lower c_γ/a_γ and $c_{\alpha 2}/a_{\alpha 2}$ ratios obtained for the (Zr + Hf)- and Zr-containing alloys contributed to the decrease and the increase in the creep resistance, respectively. The fact that the (Zr + Hf)- and Zr-containing alloys showed higher creep resistance than the Nb-containing alloy should be mostly attributed to the lower lattice misfits in the (Zr + Hf)- and Zr-containing alloys and the higher solution hardening due to doping with Zr + Hf and Zr. Therefore, the impact of alloying on the creep resistance in the β-solidifying γ-TiAl alloys should be considered taking into account the changes of the lattice parameters of the γ and α_2 phase, which have the influence on physical factors affecting the creep behavior.

Keywords creep resistance, intermetallic γ-TiAl alloys, lattice parameters, lattice misfit, microstructure

1. Introduction

Intermetallic alloys based on the γ-TiAl+α_2-Ti_3Al phases (hereafter called as γ-TiAl alloys) are lightweight high-temperature materials, which have recently been used in aircraft engines instead of nickel base superalloys (Ref 1-3). However, the production technologies of γ-TiAl alloys are still rather expensive, and further improvements in processing methods are required to reduce the cost of γ-TiAl production. Another desire of manufacturers is to increase the heat-resistant properties of γ-TiAl alloys while maintaining acceptable ductility and processability. To meet these requirements so-called β-solidifying alloys typically doped with Nb, Mo and B were developed (Ref 4-10). In contrast to peritectically solidifying alloys, the γ-TiAl alloys solidifying solely through the β phase and doped with the indicated elements have better chemical homogeneity, refined as-cast structure free of sharp casting texture and better hot deformability (Ref 8-10). However, alloying with Nb and especially with Mo, which is known as a strong β-stabilizing element in Ti- and TiAl-based alloys, leads to formation of the β(β_o) phase. This phase in the ordered condition is brittle and only elastically deformed at room temperature (Ref 11) limiting the room temperature ductility. In addition, the presence of the β(β_o) phase causes undesirable phase transformations during exposure at potential operating temperatures (Ref 12-14). Therefore, it seems to be reasonable to replace Nb and Mo by other substitution elements having a lower β stabilizing effect and a high solubility in the γ-TiAl and α_2-TiAl phase.

Our previous investigation revealed that γ-TiAl alloys based on the Ti-44Al-0.2B alloy doped with Zr and Zr + Hf demonstrated appreciably higher creep resistance than the alloy doped with Nb and the base alloy while maintaining near the same ductility below the brittle-ductile transition temperatures (Ref 15). Higher creep resistance resulted from alloying with Zr + Hf and Zr vs. Nb was ascribed to stronger solid solution hardening due to larger atomic radii of Zr and Hf and to different partitioning behaviors of the alloying elements. Apparently, there was one more reason of different creep properties of the alloys doped with Nb, Zr and Zr + Hf. Neumeier et al. have recently demonstrated that alloying with Zr instead of Nb decreased the γ(TiAl)/α_2(Ti_3Al) lattice misfits (Ref 16). This should reduce coherency stresses causing dislocation emission from the γ/α_2 interfaces and increase the creep resistance of a lamellar γ+α_2 structure. This factor should also play a certain role in case of a duplex structure.

V.M. Imayev, N.Y. Parkhimovich, D.M. Trofimov, and **R.M. Imayev**, Institute for Metals Superplasticity Problems of Russian Academy of Sciences (IMSP RAS), Ufa, Russian Federation. Contact e-mail: vimayev@mail.ru.

As is known, the crystallographic relationship between the γ and α_2 phase in γ-TiAl alloys obeys the Blackburn orientation relationship:

$$(0001)_{\alpha 2}\left|\left|\{111\}_{\gamma} and \left\langle 11\bar{2}0\right\rangle_{\alpha 2}\right|\right| < 1\bar{1}0]_{\gamma} \quad \text{(Eq 1)}$$

There are slight differences in the interatomic distances in the close-packed directions of the γ and α_2 phase inducing coherent or residual stresses (Ref 3, 17). Since the γ <110] and γ <101] directions are not equivalent in the γ phase having the $L1_0$ superlattice, the lattice misfits between the parallel $\alpha_2(0001)$ and γ{111} planes in γ <110] and γ <101] directions (ε_{110} and ε_{101}) of the γ phase are different and expressed as follows (Ref 16):

$$\varepsilon_{110} = \frac{a_{\alpha 2}}{\sqrt{2 \cdot \alpha_{\gamma}^2}} - 1 \quad \text{(Eq 2)}$$

$$\varepsilon_{101} = \frac{a_{\alpha 2}}{\sqrt{a_{\gamma}^2 + c_{\gamma}^2}} - 1 \quad \text{(Eq 3)}$$

In the present work, the effect of Nb, Zr and Zr + Hf on the lattice parameters of the β-solidifying alloys based on Ti-44Al-0.2B was investigated. The tetragonal distortion (c_{γ}/a_{γ}), the $c_{\alpha 2}/a_{\alpha 2}$ ratio of the α_2 phase and the lattice misfits calculated by Eq 2 and 3 were determined for the alloys. As in our previous work (Ref 15), the same processing route and similar duplex structures were obtained in the alloys. This allowed us to exclude the effect of different microstructures on the lattice parameters and to define the effect of the alloying elements. The obtained results were compared with the creep properties of the alloys in the duplex conditions.

Generally speaking, the present work aims at partial or complete replacement of Nb and Mo as the basic alloying elements in the β-solidifying γ-TiAl alloys by Zr and Hf having a smaller β-stabilizing effect, larger atomic radii and a high solubility in the γ-TiAl and α_2-Ti_3Al phase. To reach this goal, a better understanding of the influence of these elements on the lattice parameters of the intermetallic phases affecting different physical processes (such as dislocation glide, dislocation emission from the γ/α_2 interfaces etc.) and the creep behavior is required.

2. Materials and Experimental

The following γ-TiAl alloys were studied (at.%): Ti-44Al-0.2B (base composition), Ti-44Al-5Nb-0.2B, Ti-44Al-5Zr-0.2B and Ti-44Al-2.5Zr-2.5Hf-0.2B (hereinafter designated as BC, BC-Nb, BC-Zr and BC-(Zr + Hf), respectively). The alloys were produced via arc-melting as ingots with an approximate weight of 100 g. The ingots were remelted many times to attain good chemical homogeneity. The ingot compositions measured by energy dispersive x-ray (EDS) analysis were found to be very close to the nominal compositions.

The as-cast alloys were subjected to upset forging at T = 950 °C and low strain rates as described in detail elsewhere (Ref 15). The forged alloys were subjected to the same heat treatment, which included annealing at T = 1250 °C (2 h), followed by furnace cooling and at T = 900 °C (4 h). From the forged and heat-treated workpieces, the specimens for creep testing were prepared by spark cutting and mechanical grinding. The creep tests were carried out at T = 700 °C as described in Ref 15. The minimum creep rates were determined for the alloys from these creep tests and compared to the lattice misfits.

Scanning electron microscopy (SEM) in the back-scattering electron (BSE) mode was carried out in a Mira-3 Tescan

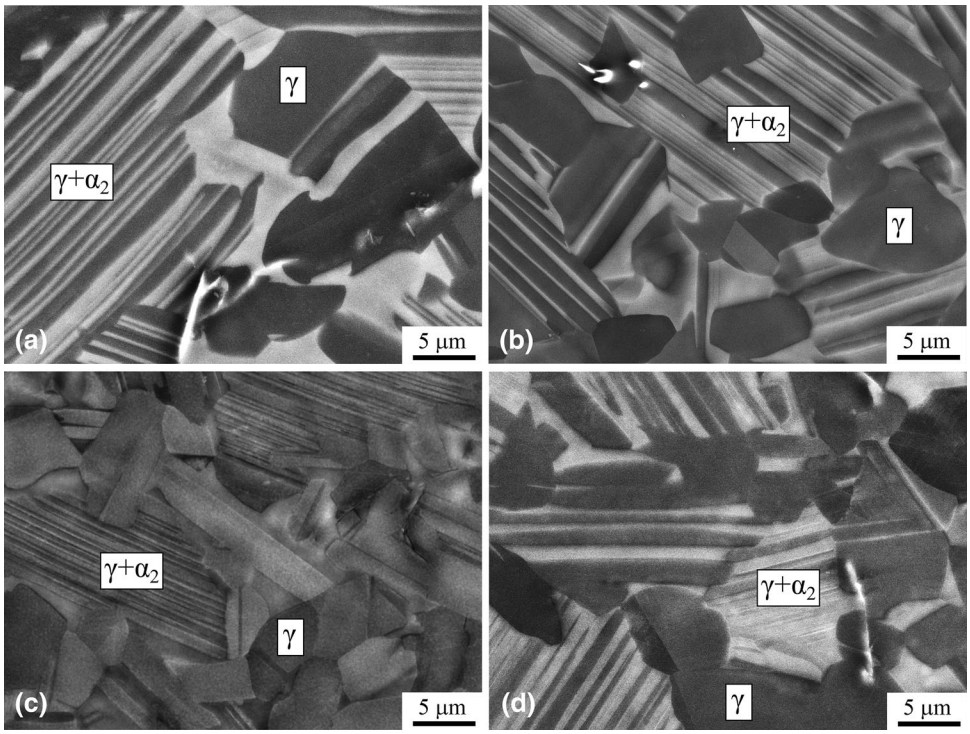

Fig. 1 BSE images of the (a) BC, (b) BC-Nb, (c) BC-Zr and (d) BC-(Zr + Hf) alloys in the duplex conditions

microscope. X-ray diffraction (XRD) analysis was carried out using *Cu-K*$_\alpha$ radiation. The lattice parameters were measured taking into consideration two different samples per alloy, and the mean lattice parameters were taken into account. The tetragonal distortion of the γ unit cell (c_γ/a_γ ratio) was calculated using the (002) and (200) peaks. The $c_{\alpha 2}/a_{\alpha 2}$ ratio of the α_2 phase was calculated using the $(2\bar{1}\bar{1}0)$ and (0002) peaks. The lattice misfits are calculated using Eq 2 and 3.

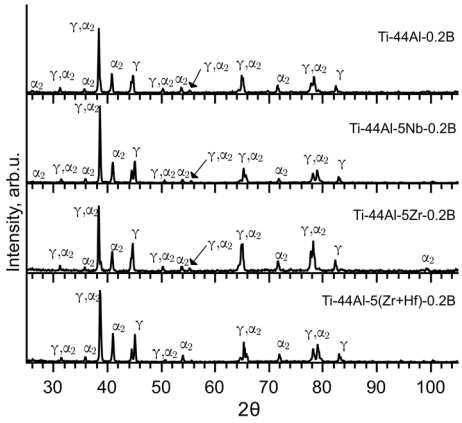

Fig. 2 XRD patterns obtained for the investigated alloys in the duplex conditions

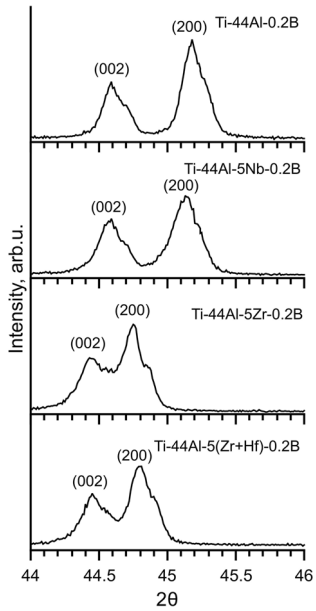

Fig. 3 XRD patterns obtained for the investigated alloys in the range of 2Θ=44-46° at room temperature

3. Results

BSE images of the alloys after upset forging and heat treatment are shown in Fig. 1. The microstructures were significantly refined after processing, and duplex structures with very similar microstructural parameters were obtained in the alloys (Ref 15). Figure 2 represents XRD patterns obtained for the alloys. The γ-TiAl and α_2-Ti_3Al were detected in the alloys. The β(β_o) phase was not revealed that is consistent with the BSE images.

Figure 3 shows the XRD patterns corresponding to the range of 44-46°. The comparison of the patterns shows that the distance between the 002 and 200 peaks of the γ phase is smaller in the BC-Zr and BC-(Zr + Hf) alloys as compared to that in the BC and BC-Nb alloys. This indicates that the tetragonal γ phase became closer to cubic in the BC-Zr and BC-(Zr + Hf) alloys.

Table 1 and Fig. 4 show the lattice parameters of the γ and α_2 phase and the calculated values of the tetragonal distortion c_γ/a_γ of the γ unit cell and the $c_{\alpha 2}/a_{\alpha 2}$ ratio of the α_2 unit cell obtained for the alloys at room temperature. In comparison with the BC alloy, doping with Nb insignificantly changed the lattice parameters of both phases in the BC-Nb alloy. This should be ascribed to the fact that the size difference between Ti and Nb atoms is not more than 0.2% (Ref 3) (taking into account that Nb occupies only the Ti sublattice in γ-TiAl alloys). Therefore, the c_γ/a_γ and $c_{\alpha 2}/a_{\alpha 2}$ ratios in the BC-Nb alloy were near the same as in the BC alloy.

Alloying with Zr and Zr + Hf led to a small increase in the c_γ and $c_{\alpha 2}$ parameters and to a more appreciable increase in the a_γ and $a_{\alpha 2}$ parameters. Note that Ti and Al atoms are arranged in layers in the γ-TiAl phase (superlattice $L1_0$). Zr and Hf atoms having significantly larger radii than Ti (0.160 and 0.159 nm against 0.145 nm) and occupy only or preferentially the Ti sublattice in layers (Ref 3) and, therefore, change first of all the a_γ parameter. In the α_2 phase (superlattice $D0_{19}$), the basal planes (0001) contain not only Ti atoms, but also Al atoms and, therefore, the effect of larger radii of Zr and Hf occupying the Ti sublattice led to a smaller increase in the $a_{\alpha 2}$ parameter as compared to the a_γ parameter. The different influence of Nb, Zr and Zr + Hf on the lattice parameters of the γ and α_2 phase can be also associated with a different partitioning behavior of Nb, Zr and Hf. Partitioning preference is known to be near equal or $\gamma > \alpha_2$ for Nb, strongly $\gamma > \alpha_2$ for Zr and near equal for Hf (Ref

Table 1 Average lattice parameters of the γ and α_2 phase and the calculated c_γ/a_γ and $c_{\alpha 2}/a_{\alpha 2}$ ratios obtained for the alloys at room temperature

Alloy	a_γ, Å	c_γ, Å	c_γ/a_γ	$a_{\alpha 2}$, Å	$c_{\alpha 2}$, Å	$c_{\alpha 2}/a_{\alpha 2}$	c_γ/a_γ (Ref 16)	$c_{\alpha 2}/a_{\alpha 2}$ (Ref 16)
BC	4.0107	4.0603	1.0124	5.754	4.6365	1.6116	1.02 (Ti-44Al) FL	1.6106
BC-Nb	4.0146	4.0611	1.0116	5.7558	4.6496	1.6156	1.012 (Ti-44Al-5Nb) FL	1.6202
BC-Zr	4.0463	4.0743	1.0069	5.7757	4.639	1.6064	1.0061 (Ti-44Al-5Zr) FL	1.6029
BC-(Zr + Hf)	4.0419	4.0722	1.0075	5.7804	4.6429	1.6064	…	…

FL fully lamellar conditions.

15, 16, 18). As a result, alloying with Zr and Zr + Hf provided an appreciable decrease in the tetragonal distortion c_γ/a_γ of the γ unit cell and a smaller decrease in the $c_{\alpha 2}/a_{\alpha 2}$ ratio of the α_2 unit cell. Thus, in terms of crystal symmetry, the tetragonal γ phase became closer to cubic and the α_2 phase became farther from the ideal hexagonal close-packed lattice in the BC-Zr and BC-(Zr + Hf) alloys, whereas the c_γ/a_γ and $c_{\alpha 2}/a_{\alpha 2}$ ratios were found near the same in the BC and BC-Nb alloys (Fig. 4).

The comparison with data obtained in Ref 16 shows a good agreement for the Nb- and Zr-containing alloys and some difference of the c_γ/a_γ value in the case of the base alloy, which is probably associated with refined duplex-type structure in the BC alloy in contrast to the coarse lamellar structure obtained in Ti-44Al (Table 1).

Table 2 shows the lattice misfits in the duplex conditions of the alloys determined in both crystallographic directions. The lattice misfits decreased from the BC alloy to the BC-Nb and then to the BC-(Zr + Hf) and BC-Zr alloy. Note that the lattice misfits obtained for the Nb- and Zr-containing alloys in Ref 16 were similar to those obtained in the present work (Table 2). Some difference was revealed for the BC alloy and the binary alloy. As in the case of the c_γ/a_γ ratio, this may be associated with a coarse lamellar structure obtained in the Ti-44Al alloy in contrast to the refined duplex structure obtained in the Ti-44Al-0.2B alloy.

As is known (Ref 3), the lattice misfit induces coherency stresses promoting dislocation emission from the γ/α_2 interfaces under creep testing. This factor is especially important for a fully lamellar condition but should be also taken into consideration in the case of a duplex condition. Figure 5 shows the minimum creep rates at 700 °C taken from our previous work (Ref 15) as a function of the lattice misfit averaged over the γ <110] and γ <101] directions for the alloys in the duplex conditions. The highest creep resistance showed the BC-(Zr + Hf) and BC-Zr alloys, followed by the BC-Nb and BC alloys. Generally speaking, the smaller lattice misfit should decrease the minimum creep rate. However, there are also other factors, which are discussed below, having an impact on the creep resistance. Therefore, the dependencies of the minimum creep rate on the lattice misfit are nonmonotonic (Fig. 5).

4. Discussion

The obtained results show that alloying with Zr and Zr + Hf has a rather tangible influence on the lattice parameters and the resulting c_γ/a_γ and $c_{\alpha 2}/a_{\alpha 2}$ ratios (the $c_{\alpha 2}/a_{\alpha 2}$ ratio to a lesser extent) in the γ and α_2 phase, whereas alloying with Nb leads only to insignificant changes in the lattice parameters and the resulting c_γ/a_γ and $c_{\alpha 2}/a_{\alpha 2}$ ratios in comparison with the BC alloy. However, the c_γ/a_γ and $c_{\alpha 2}/a_{\alpha 2}$ ratios and the lattice misfits do not show definite correlations with the creep resistance of the investigated alloys because a number of factors influence the creep resistance.

The smaller the c_γ/a_γ ratio (closer to 1), the easier the dislocation glide in the γ phase. Therefore, a lower c_γ/a_γ ratio obtained for the BC-Zr and BC-(Zr + Hf) alloys should have a negative impact on the creep resistance. Reduced $c_{\alpha 2}/a_{\alpha 2}$ ratio, on the contrary, should hinder the movement of dislocations in the α_2 phase that can have a slight positive influence on the creep resistance. The smaller the lattice misfits, the higher creep resistance. As mentioned, Zr and Hf have larger atomic radii than Nb. This provides higher solution hardening that was confirmed by tensile properties (Ref 15). Higher solution hardening should have a positive impact on the creep resistance.

Alloying with Nb slows down the diffusivity stronger than with Zr (Ref 19). There is no data on Hf but a high melting point of Hf should slow down the diffusivity and have a

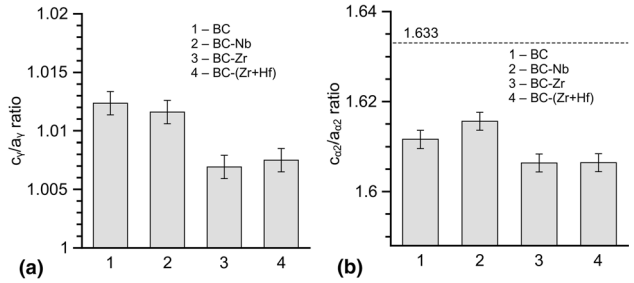

Fig. 4 (a) Tetragonal distortion c_γ/a_γ of the γ unit cell and (b) the $c_{\alpha 2}/a_{\alpha 2}$ ratio of the α_2 unit cell obtained for the alloys at room temperature. The dotted line indicates the $c_{\alpha 2}/a_{\alpha 2}$ ratio corresponding to the ideal hexagonal close-packed lattice

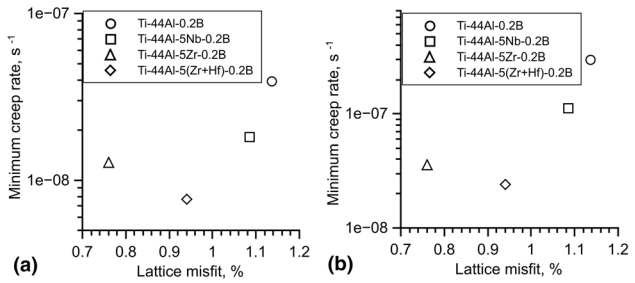

Fig. 5 Minimum creep rate for the alloys at (a) 700 °C / 250 MPa and (b) 700 °C / 350 MPa as determined in Ref 15, as a function of the lattice misfit averaged over the γ <110] and γ <101] directions for the investigated alloys with the duplex structures

Table 2 Lattice misfits determined for the alloys in the duplex conditions in both crystallographic directions

Alloy	ε_{110}, %	ε_{101}, %	ε_{110}, % (Ref 16)	ε_{101}, % (Ref 16)
BC	1.45	0.82	2.1 (Ti-44Al, FL)	1.12 (Ti-44Al, FL)
BC-Nb	1.38	0.79	1.33 (Ti-44Al-5Nb, FL)	0.7 (Ti-44Al-5Nb, FL)
BC-Zr	0.93	0.59	1.07 (Ti-44Al-5Zr, FL)	0.75 (Ti-44Al-5Zr, FL)
BC-(Zr + Hf)	1.13	0.75	…	…

FL fully lamellar conditions.

Table 3 Qualitative assessment of the effect of Nb, Zr and Zr + Hf on the creep resistance of the BC alloy via different physical factors (designated as "+", "±" and "−")

Physical factors	The qualitative influence on the creep resistance		
	Nb	Zr	Zr + Hf
The tetragonal distortion c_γ/a_γ of the γ unit cell	+	−	−
The $c_{\alpha 2}/a_{\alpha 2}$ ratio of the α_2 unit cell	−	+	+
The γ/α_2 lattice misfits	−	+	+
Solid solution hardening	−	+	+
Effect of alloying on diffusivity	+	−	±
Partition between the γ and α_2 phase	±	+	±
Solubility in the γ and α_2 phase (the formation of additional phases)	±	+	+
β-stabilizing effect	±	+	±

positive impact on the creep resistance. The partitioning preference is different for Nb, Zr and Hf (Ref 15, 16, 18). The strong $\gamma > \alpha_2$ preference for Zr should be favorable for creep resistance in a duplex condition.

The presence of Nb, as mentioned, can lead to phase transformations during exposure at high temperatures (Ref 12-14), which should have a negative impact on the creep resistance. Zr and Zr + Hf have a high solubility in the γ and α_2 phase and should not lead to formation of undesirable phases. At last, Nb and Zr + Hf gave weak and approximately equal β-stabilization effect and slightly higher than Zr (Ref 15). A weaker β-stabilization effect of Zr should have a positive impact on the creep resistance. Table 3 summarizes the mentioned factors and gives the qualitative assessment of their influence on the creep resistance of the alloys under study.

Thus, the effect of Nb, Zr and Zr + Hf on the creep resistance of β-solidifying γ-TiAl alloys should be considered through the effect of the alloying elements on different physical factors. Apparently, some of them, such as the γ/α_2 lattice misfits, solution hardening, effect of alloying on the tetragonal distortion of the γ unit cell and the diffusivity, are more significant than the others. Considering these factors as having near the same influence on the creep resistance, one can conclude that the number of positive factors is higher for the BC-Zr and BC-(Zr + Hf) alloys than for the BC-Nb alloy. Therefore, the BC-Zr and BC-(Zr + Hf) alloys demonstrated a better creep resistance (a lower minimum creep rate) than the BC-Nb alloy.

5. Conclusions

The influence of alloying with 5 at.% Nb, 5 at.% Zr and 2.5 at.% Zr + 2.5 at.% Hf on the lattice parameters of the Ti-44Al-0.2B base alloy was studied by XRD technique. Before XRD analysis near the same duplex structures were obtained in the alloys. The obtained results suggest that the effect of alloying on the creep resistance should be considered taking into account the changes in the lattice parameters, which have the influence on different physical processes and the creep behavior.

(1) The c_γ/a_γ ratio in the alloys was the highest in the base alloy, followed by the Nb-, (Zr + Hf)- and Zr-containing alloy.
(2) The $c_{\alpha 2}/a_{\alpha 2}$ ratio in the alloys was the highest in the Nb-containing alloy, followed by the base alloy and the Zr- and (Zr + Hf)-containing alloy.
(3) The lattice misfits in the alloys were the highest in the base alloy, followed by the Nb-, (Zr + Hf)- and Zr-containing alloy.
(4) The lower c_γ/a_γ ratios obtained for the (Zr + Hf)- and Zr-containing alloys should promote easier dislocation glide in the γ phase and most likely played a negative role in the creep resistance. On the contrary, the lower $c_{\alpha 2}/a_{\alpha 2}$ ratios obtained for the (Zr + Hf)- and Zr-containing alloys should hinder dislocation glide in the α_2 phase that most likely played a positive role in the creep resistance. The fact that the Ti-44Al-5(Zr + Hf)-0.2B and Ti-44Al-5Zr-0.2B alloys demonstrated better creep resistance than the Ti-44Al-5Nb-0.2B alloy should be mostly contributed to the different lattice misfits in the alloys and the higher solid solution hardening due to doping with Zr + Hf and Zr.
(5) The lattice misfit itself is an important factor having a strong impact on the creep resistance of the β-solidifying γ-TiAl alloys even in case of a duplex structure. The larger the lattice misfit, the lower the creep resistance. For the (Zr + Hf)-containing alloy this tendency was slightly distorted because of Hf, which being a refractory element, apparently contributed to a decrease in the diffusivity.

Acknowledgments

The work was supported by the Ministry of Science and Higher Education of the Russian Federation according to the State Assignment of the IMSP RAS (No. AAAA-A17-117041310215-4).

References

1. B.P. Bewlay, S. Nag, A. Suzuki, and M.J. Weimer, TiAl Alloys in Commercial Aircraft Engines, *Mater. High Temps.*, 2016, **33**, p 549–559.
2. P. Janschek, Wrought TiAl Blades, *Mater. Today: Proc.*, 2015, **2S**, p S92–S97.
3. F. Appel, J.D.H. Paul, and M. Oehring, *Gamma Titanium Aluminide Alloys: Science and Technology*, Wiley-VCH, Weinheim, 2011

4. V. Küstner, M. Oehring, A. Chatterjee, V. Güther, H.-G. Brokmeier, H. Clemens, et al. *Gamma titanium Aluminides 2003*. Y. -W. Kim, H. Clemens, A. H. Rosenberger Ed. Warrendale (PA), TMS, 2003, p 89-96
5. Y. Jin, J.N. Wang, J. Yang, and Y. Wang, Microstructure Refinement of Cast TiAl Alloys by β-solidification, *Scr. Mater.*, 2004, **51**, p 113–117.
6. R.M. Imayev, V.M. Imayev, M. Oehring, and F. Appel, Alloy Design Concepts for Refined Cast and Wrought Gamma Titanium Aluminide Based Alloys, *Intermetallics*, 2007, **15**, p 451–460.
7. V.M. Imayev, R.M. Imayev, T.I. Oleneva, and T.G. Khismatullin, Microstructure and Mechanical Properties of the Intermetallic Alloy Ti-45Al-6(Nb, Mo)-0.2B, *Phys. Met. Metallogr.*, 2008, **106**(6), p 641–648.
8. H. Clemens, W. Wallgram, S. Kremmer, V. Güther, A. Otto, and A. Bartels, Design of Novel β-solidifying TiAl Alloys with Adjustable β/B2-phase Fraction and Excellent Hot Workability, *Adv. Eng. Mater.*, 2008, **10**, p 707–713.
9. H. Clemens and S. Mayer, Design, Processing, Microstructure, Properties, and Applications of Advanced Intermetallic TiAl Alloys, *Adv. Eng. Mater.*, 2013, **15**, p 191–215.
10. V. Imayev, R. Imayev, T. Khismatullin, T. Oleneva, V. Gühter, and H.-J. Fecht, Microstructure and Processing Ability of β-Solidifying TNM-Based γ-TiAl Alloys, *Mater. Sci. Forum*, 2010, **638–642**, p 235–240.
11. P. Erdely, P. Staron, E. Maawad, N. Schell, H. Clemens, and S. Mayer, Lattice and Phase Strain Evolution During Tensile Loading of an Intermetallic, Multi-phase γ-TiAl Based Alloy, *Acta Mater.*, 2018, **158**, p 193–205.
12. Z.W. Huang and T. Cong, Microstructural Instability and Embrittlement Behaviour of an Al-lean, High-Nb γ-TiAl-based Alloy Subjected to a Long-term Thermal Exposure in air, *Intermetallics*, 2010, **18**, p 161–172.
13. S. Bolz, M. Oehring, J. Lindemann, F. Pyczak, J. Paul, A. Stark, T. Lippmann, S. Schrüfer, D. Roth-Fagaraseanu, A. Schreyer, and S. Weiß, Microstructure and Mechanical Properties of a Forged β-solidifying γ TiAl Alloy in Different Heat Treatment Conditions, *Intermetallics*, 2015, **58**, p 71–83.
14. M. Kastenhuber, B. Rashkova, H. Clemens, and S. Mayer, Effect of Microstructural Instability on the Creep Resistance of an Advanced Intermetallic γ-TiAl Based Alloy, *Intermetallics*, 2017, **80**, p 1–9.
15. V.M. Imayev, A.A. Ganeev, D.M. Trofimov, NJu. Parkhimovich, and R.M. Imayev, Effect of Nb, Zr and Zr + Hf on the Microstructure and Mechanical Properties of β-Solidifying γ-TiAl Alloys, *Mater. Sci. Eng. A*, 2021, **817**, p 141388.
16. S. Neumeier, J. Bresler, C. Zenk, L. Haußmann, A. Stark, F. Pyczak, and M. Göken, Partitioning Behavior of Nb, Ta and Zr in Fully Lamellar $\gamma+\alpha_2$ Titanium Aluminides and its Effect on the Lattice Misfit and Creep Behavior, *Adv. Eng. Mater.*, 2021, **23**, p 2100156.
17. A. Chauniyal and R. Janisch, Influence of Lattice Misfit on the Deformation Behaviour of α_2/γ Lamellae inTiAl Alloys, *Mater. Sci. & Eng. A*, 2020, **796**, p 140053.
18. R. Kainuma, Y. Fujita, H. Mitsui, I. Ohnuma, and K. Ishida, Phase Equilibria Among α(hcp), β(bcc) and $\gamma(L1_0)$ Phases in Ti-Al Base Ternary Alloys, *Intermetallics*, 2000, **8**, p 855–867.
19. Chr Herzig, T. Przeorski, M. Friesel, F. Hisker, and S. Divinski, Tracer Solute Diffusion of Nb, Zr, Cr, Fe, and Ni in γ-TiAl: Effect of Preferential Site Occupation, *Intermetallics*, 2001, **9**, p 461–472.